Electr Eng
DOI 10.1007/s00202-017-0535-1

ORIGINAL PAPER

A new strategy for battery and supercapacitor energy management for an urban electric vehicle

Idris Azizi[1] · **Hammoud Radjeai**[1]

Received: 6 October 2016 / Accepted: 10 April 2017

Abstract A new strategy of energy management between battery and supercapacitors for an urban electric vehicle is suggested in this paper. These two sources are connected in parallel to the DC bus through two bidirectional DC–DC converters enabling separate control over the power flow of each source. Vehicle dynamics with load torque applied on the shaft motor is to be considered. This strategy of energy management permits dividing energy between the two sources depending on the state of charge of each source as well as on the vehicle displacement state such as stopping, acceleration, cruising down and uphill, and deceleration. The aim of the proposed strategy is the best use of energy through maximizing the use of SCs by transferring energy from batteries to SCs during the standstill phase or when the load applied to the vehicle is small; supercapacitors will then be ready in critical situations such as rapid acceleration or in high hills climbing. In order to validate the control design and evaluate our energy management strategy performance, a simulation of an urban hybrid electric vehicle movement with the Matlab/Simulink software is implemented.

Keywords Energy management · Battery · Supercapacitor · Bidirectional converter · Field orientation control · Vehicle dynamics

1 Introduction

As noise and polluting gases as well as fuel consumption keep steadily rising, interest in electric vehicles (EVs) is constantly renewed. EV is one of the solutions recommended by vehicle manufacturers and research organizations to gradually replace conventional vehicles especially in city centres [1]. Computer modeling and simulation can be used to reduce the expense and length of the design cycle of EVs by testing configurations and energy management strategies before prototype construction begins. Interest in EV and hybrid EV grew in the 1970's leading to the development of several prototypes [2].

With revolutionary contributions of power electronics and energy storage systems, electric drive trains are totally or partially replacing gradually internal combustion engine (ICE) in standard vehicles despite several shortcomings [3]. EV's major drawback is the energy storage issue. Many researches have been conducted to increase electric driving range, improve efficiency, decrease cost and makes EV competitive with conventional vehicles in the market [3,4].

Actually reliable energy sources such as batteries, fuel cells, supercapacitors and high speed flywheels seem to offer the best potentialities for EV. As for now, advances in flywheels technology are not in pace with EV development [4]. Fuel cells have high energy density and clean energy properties but have poor response time to instantaneous power demands, due to air delivery system low response time. Besides they are costly and incapable of accepting the regenerative energy during EV braking or downhill driving [3,4]. On the other hand supercapacitors (SCs) offer several gains over electrolytic capacitors amid which high energy, efficiency, as well as extended durability [5]. Batteries (BTs) remain as the main energy storage devices in transportation applications. In spite of their relatively high energy density, they are characterized by a low power density depending on the battery type. Furthermore, they have a relatively short life cycle and low dynamics [6].

✉ Idris Azizi
i.azizi@univ-setif.dz

[1] Automatic Laboratory (LAS), Faculty of Technology, Setif -1- University, Setif, Algeria

Published online: 24 April 2017

Finally one can conclude that available energy sources are not ideal and offer either high specific power (HSP) or high specific energy (HSE). While both of these qualities are required, they are yet to be found in one type of energy source. HSE allows for acceptable driving range, whereas HSP is needed for rapid accelerations and hill climbing. It is therefore imperative to use different type of sources with a sound energy flow strategy management [7].

Power sharing between supercapacitors and batteries is a promising solution for improving system performance due to the dynamic behavior of the SCs and their long life which can help preventing battery overstress [8,9].

Converting kinetic energy available during braking into electrical energy supplied to an energy storage system is a formidable way to boost range capabilities of EVs and to reduce their energy storage source sizes [10]. In this way, reference [10] pointed out that the regenerative braking can increase the EV range in the interval of 8–25%.

Experiment in reference [11] indicates that hybrid power system can improve the efficiency of braking energy recovery and decreases the demanding power of the battery. It also shows that the braking energy recovery rate of hybrid power system is 11% higher than of the battery system alone, the main reason being that SC has ability to charge very quickly. Authors in reference [9] proposed an advanced energy management system based on the adequate discharge of the supercapacitor bank in order to utilize all the energy available from the regenerative braking but the state of charge (SOC) of the battery bank never increases; due to the fact that the SC is the unique active source during the regenerative braking. In the reference [8], the authors presented a power-sharing method between supercapacitors and lead-acid battery in a 500-KVA rated uninterruptible power supply (UPS) but they did not take into account the regenerative braking mode. Another remarkable work is given in reference [12] where the authors showed that an H∞ robust controller out-performed the traditional PID regulator in many respects including stability, error, responding speed and driving distance between battery charges.

In this work, we present a new energy management strategy, which can perform an appropriate exchange of power between the load and the two sources of the energy storage system of the vehicle by considering the two modes of operation: motor and regenerative braking modes for a known displacement of an urban vehicle. Simulation results show that both batteries and supercapacitors benefit from the regenerative braking mode while the state of supercapacitors charge remains at a high level yielding improved electric vehicle range and extended battery lifetime.

2 System modeling and control strategy

The power train of the electric vehicle consists of an energy storage system, two bidirectional dc–dc converters, and motor drive. The electric power train was dimensioned taking into account the physical characteristics of the EV specified in Table 1.

The system architecture under study is given in Fig. 1.

Table 1 Parameters of vehicle body [13]

Parameter	Value	Parameter	Value
Masse of vehicle M (kg)	1150	Vehicle frontal area A_f (m^2)	2.5
Transmission ratio i	10	Air density ρ (kg/m^3)	1.28
Aerodynamic drag coefficient C_d	0.32	Wheel radius r (m)	0.33
Tire rolling resistance coefficient μ	0.015	Earth gravity g (m/s^2)	9.81

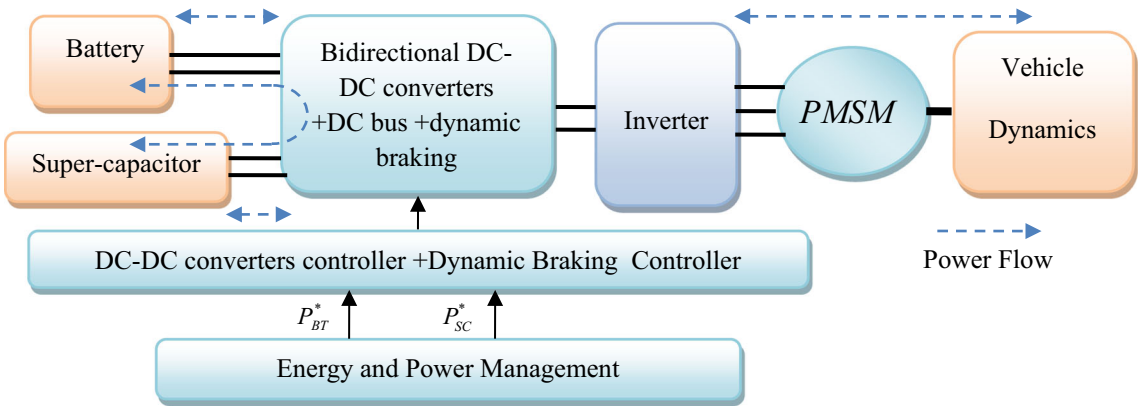

Fig. 1 Block diagram of the proposed system

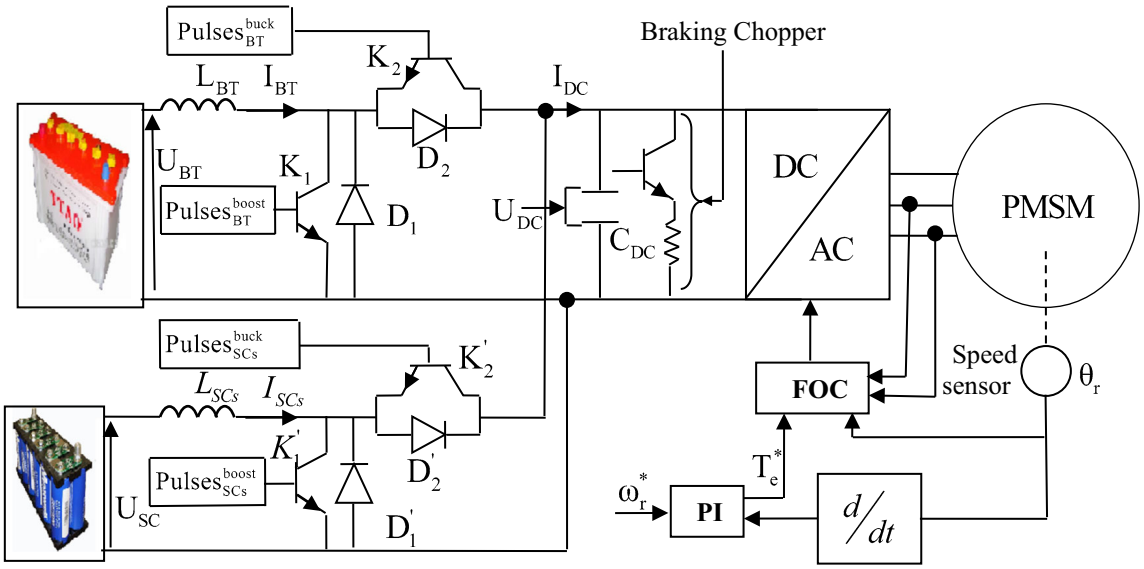

Fig. 2 Schematics of the EV electric system

2.1 Energy storage system (ESS)

The proposed energy management system (EMS) was developed considering a hybrid energy storage system that consists of a battery bank and supercapacitor bank. In MATLAB library, the blocks of battery and supercapacitor implement generic models parameterized to represent most popular types of rechargeable batteries and supercapacitors [14,15]. For this study we used a lithium battery as the main energy storage device with a rated voltage of 278 V, and a rated capacity of 90 Ah. The auxiliary source ratings (Supercapacitors) are 240 V voltage and a capacitance of 23.9 F.

2.2 DC–DC converters

Two DC–DC converters are linked to the same DC-Link, one manages the battery power flow and the other manages the SCs power flow, as shown in Fig. 2. Energy transfer is enabled between sources and load and back in the aforementioned structure as well as from one source to another independently of energy flow direction. DC-link current, I_{DC}, can be positive or negative whereas voltage across the DC bus is always positive. The two parallel DC–DC converters that interface the SCs and the battery with the DC-Link give a good flexibility power management either when energy flow to DC-Link rising the voltage level which is boost behavior, or when energy flows from DC-Link to sources showing a typical buck behavior. In boost-mode, $(K_1/K_1^{'})$ and $(D_2/D_2^{'})$ are active. In the buck-mode, $(K_2/K_2^{'})$ and $(D_1/D_1^{'})$ are active [16,17]. The dynamic braking chopper is used to absorb the energy produced during motor deceleration or when the load torque tends to accelerate the motor, this occurs when the battery and supercapacitors are fully charged. Power inductors L_{BT} and L_{SCs} play an important role in the overall performance of the system, limiting current oscillations magnitude; a smoothing inductance is placed in series with each source circuit while a good choice of capacity C_{DC} justifies good damping of ripple of DC bus [18]. DC bus voltage (U_{DC}) control is used for the purpose of maintaining a constant reference value by controlling the process of loading and unloading of the capacitor. The power flow in the DC-link capacitor is described by Eq. (1):

$$P_{DC} = C_{DC}\frac{dU_{DC}}{dt}U_{DC} = \frac{dE_{DC}}{dt} = P_{Sour} - P_{Load} \quad (1)$$

P_{DC}(W): resulted DC-link power, E_{DC}(J): energy stored in the DC-link capacitor, P_{Sour}(W): power source, P_{Load}(W): Asked power from the load, C_{DC}(F): capacitor.

The control of the DC–DC converter is realized via a cascade configuration (Fig. 3). In order to upkeep the dc bus voltage, a main voltage loop with a proportional-integral (PI) controller generates the total current reference I^*_{DC} that should be taken from the DC-link bus. This total current reference is then distributed by the EMS that generates the set points currents for all sources. The regulators of supercapacitor and battery converters are current-controllers with hysteresis regulators [19,20].

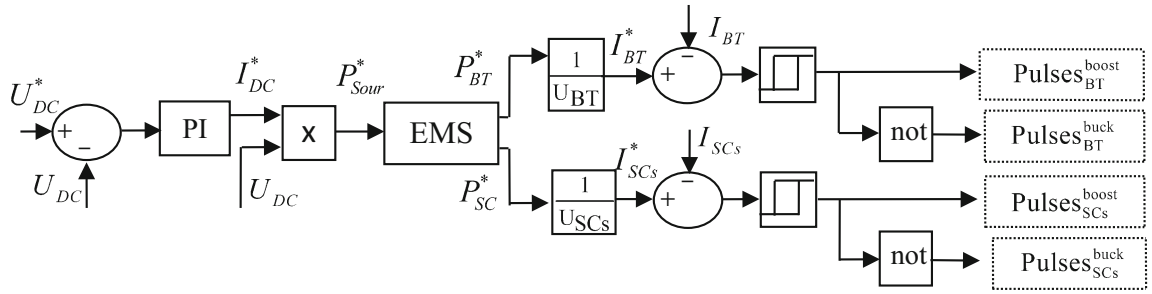

Fig. 3 Control scheme of DC–DC converters

Table 2 Parameters of PMSM

Parameter	Value	Parameter	Value
Rated power (KW)	35	Rotor inertia J (kg m^2)	0.05
Rated torque (N m)	111	Number of pole pairs p	4
Rated speed (tr/min)	3000	DC voltage (V)	560
Resistance of the stator windings $R(\Omega)$	0.05	Stator inductance L_d, L_q (mH)	0.635

2.3 Field-oriented variable-frequency PMSM drive

2.3.1 PMSM model

The permanent magnet synchronous machine (PMSM) operates in either generating or motoring mode. Motor parameters are summarized in Table 2.

The following equations expressed in the rotor reference frame describe the PMSM model [21].

2.3.1.1 Electrical system

$$\begin{cases} \frac{\mathrm{d}}{\mathrm{d}t} i_d = \frac{1}{L_d} v_d - \frac{R}{L_d} i_d + \frac{L_q}{L_d} p\omega_\mathrm{r} i_q \\ \frac{\mathrm{d}}{\mathrm{d}t} i_q = \frac{1}{L_q} v_q - \frac{R}{L_q} i_q - \frac{L_d}{L_q} p\omega_\mathrm{r} i_d - \frac{\lambda p\omega_\mathrm{r}}{L_q} \\ T_\mathrm{e} = 1.5p[\lambda i_q + (L_d - L_q) i_d i_q] \end{cases} \tag{2}$$

i_d, i_q (A) represent $d-q$ axis stator currents, v_d, v_q (V): $d-q$ axis stator voltages, λ_d, λ_q (Wb): $d-q$ axis stator fluxes, L_d, L_q stator inductances, R: resistance of the stator windings, p: number of pole pairs, ω_r (rad/s) the mechanical speed, Te (N m): electromagnetic torque, and λ(Wb): rotor magnet flux.

2.3.1.2 Mechanical System

$$\begin{cases} \frac{\mathrm{d}}{\mathrm{d}t}\omega_\mathrm{r} = \left(\frac{1}{J} T_\mathrm{e} - F\omega_\mathrm{r} - T_L\right) \\ \frac{\mathrm{d}\theta_\mathrm{r}}{\mathrm{d}t} = \omega_\mathrm{r} \end{cases} \tag{3}$$

F (N m s): the viscous friction, J(kg m^2): the rotor inertia, and θ_r (rad): the mechanical rotor angle.

2.3.2 Field-oriented control (FOC)

Figure 4 illustrates the block diagram of the FOC. The product of the mechanical rotor angle θ_r (rad) by the number of pair poles (p) gives the electrical rotor angle θ_e (rad) which is used in the conversion of the dq component of the rotor flux rotating field reference frame into abc phase variables. Derivative of mechanical angle provides the mechanical speed ω_r (rad/s). The motor speed ω_r is compared to the reference ω^*_r and the error is processed by the speed controller to produce a torque command T^*_e. The speed controller is of a PI type. The stator direct and quadrature-axis current references i^*_d and i^*_q are converted into phase current references i^*_a, i^*_b, i^*_c for the current regulators. The regulators process

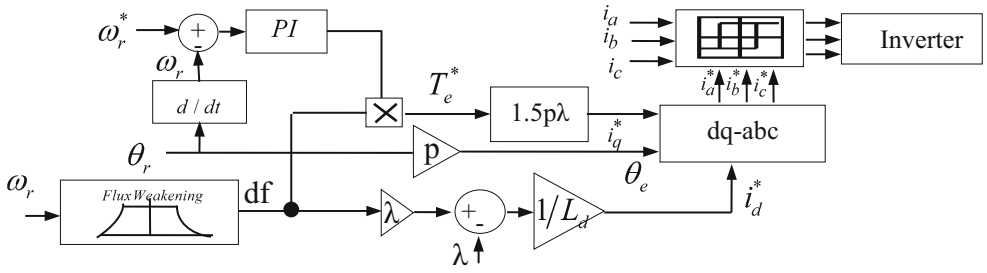

Fig. 4 Diagram of the FOC principle

the measured and reference currents to produce the inverter gating signals [22]. The equation of the flux in the $d-q$ reference is given by:

$$\begin{aligned}\lambda_d &= L_d i_d + \lambda \\ \lambda_q &= L_q i_q\end{aligned} \tag{4}$$

As the PMSM is fully controllable by the stator, the air-gap flux is weakened by the introducing of a negative current i_d which creates a flux in opposition to that of the magnets. The flux weakening used when the motor speed exceeds the nominal speed ω_0 is defined by the following nonlinearity:

$$\mathrm{df} = \begin{cases} 1 & \text{if } |\omega_\mathrm{r} \leq \omega_0| \\ \frac{\omega_0}{|\omega_\mathrm{r}|} & \text{if } |\omega_\mathrm{r}| > \omega_0 \end{cases} \tag{5}$$

3 Vehicle dynamics analysis [23,24]

3.1 Road load and tractive force

The total tractive effort is the sum of all present forces:

$$F_\mathrm{te} = F_\mathrm{roll} + F_\mathrm{aero} + F_\mathrm{gr} + F_a \tag{6}$$

The first force F_roll is called rolling resistance which is produced by the tire flattening at the roadway contact surface. The second resistance is the aerodynamic force F_aero. The third resistance force is applied when the vehicle is climbing a hill thus depending on the slope of the roadway. The fourth is called the acceleration force, it is positive when the vehicle accelerates, and negative when the vehicle decelerates.

$$\begin{cases} F_\mathrm{roll} = M \cdot g \cdot \mu \\ F_\mathrm{aero} = 0.5 \cdot \rho \cdot C_\mathrm{d} \cdot A_\mathrm{f} \cdot (v \pm v_\mathrm{wind})^2 \\ F_\mathrm{gr} = \pm M \cdot g \cdot \sin\alpha \\ F_a = \pm M_\mathrm{e} \frac{\mathrm{d}v}{\mathrm{d}t} \end{cases} \tag{7}$$

v (m/s): the vehicle speed, v: wind speed (m/s), α (rad): angle of the slope and M_e is the equivalent mass:

$$M_\mathrm{e} = \delta M \tag{8}$$

δ is the rotational inertia factor or mass factor:

$$\delta = 1 + 0.04 + 0.0025 i^2 \tag{9}$$

3.2 Motor ratings and transmission

The equation describing dynamics behavior of the electric motor, in the motor referential, is given as:

$$T_\mathrm{e} - T_\mathrm{L} = J_T \frac{\mathrm{d}\omega_\mathrm{r}}{\mathrm{d}t} \tag{10}$$

The load torque in the motor referential is given by

$$T_\mathrm{L} = \frac{T_\mathrm{Lwheel}}{i} = \frac{r}{i} F_\mathrm{R} \tag{11}$$

T_Lwheel(N m) represents load torque on the wheels, F_R(N) the resistive forces.
The vehicle global inertia moment in the motor referential is given by

$$J_T = \frac{M_\mathrm{e} r^2}{i^2}. \tag{12}$$

4 Proposal for the energy management system

Energy conversion law is used as a base for all EMS meaning that the load power needed is to be supplied by available power sources. For illustration purpose: for an ESS based on battery and SCs, energy conservation law leads to [9]:

$$P_\mathrm{Load} = P_\mathrm{Sour} = P_\mathrm{BT} + P_\mathrm{SC} \tag{13}$$

On the other hand, assuming that the sub-system consisting of the inverter and the PMSM operates with an efficiency η of 95%, the power load is calculated by:

$$P_\mathrm{load} = V_\mathrm{DC} \times I_\mathrm{DC} = \frac{1}{\eta} F_\mathrm{te} \times v \tag{14}$$

Table 3 summarizes the equations used to calculate actual powers and reference control variables.

Both operations, motor or regenerative braking modes depend on the load; if the acceleration or the slope is positive, then the load torque is positive and the vehicle operates in motor mode, otherwise it operates in regenerative braking mode. The input signals of the EMS are the SOC of the battery bank ($\mathrm{SOC_{BT}}$), SOC of the supercapacitor bank ($\mathrm{SOC_{SCs}}$), vehicle speed (v), acceleration (acc), load torque (T_L), the rated power of the battery (P_RBT), the reference source power P^*_Sour, and the load power limit P_Lm while the output signals of the EMS are the reference power of the battery(P^*_BT) and the supercapacitors(P^*_SCs) (Fig. 5a).

When the EV ignition is turned on and the vehicle is stopped, prior to an acceleration phase, one needs to fully charge the unit with more HSP (supercapacitors) from the other unit that has more HSE (battery); that is if the speed

Table 3 Power calculation for the electric system

Power source	Power calculation	Power control
DC-link	$P_\mathrm{Load} = 1/\eta F_\mathrm{te} \times v$	$P^*_\mathrm{Sour} = V_\mathrm{dc} \times I^*_\mathrm{dc}$
Battery	$P_\mathrm{BT} = V_\mathrm{BT} \times I_\mathrm{BT}$	$P^*_\mathrm{BT} = V_\mathrm{BT} \times I^*_\mathrm{BT}$
Supercapacitors	$P_\mathrm{SC} = V_\mathrm{SC} \times I_\mathrm{SC}$	$P^*_\mathrm{SC} = V_\mathrm{SC} \times I^*_\mathrm{SC}$

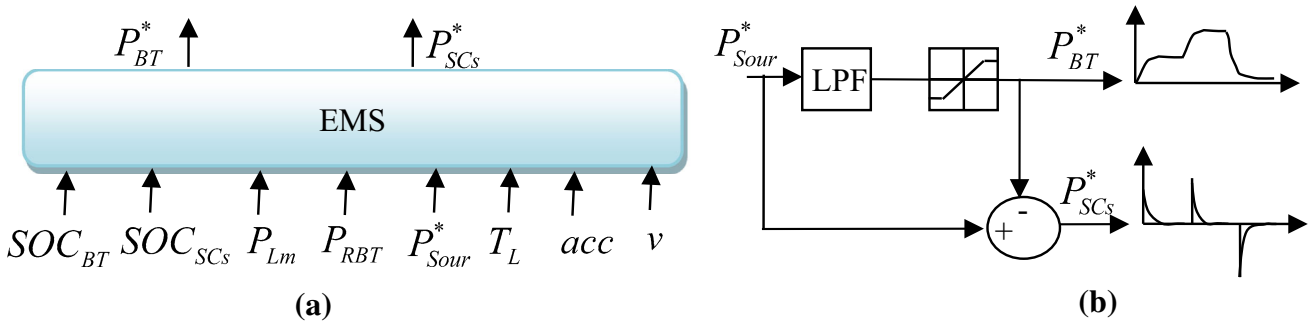

Fig. 5 **a** Inputs and outputs of EMS, **b** operating principle of LPF

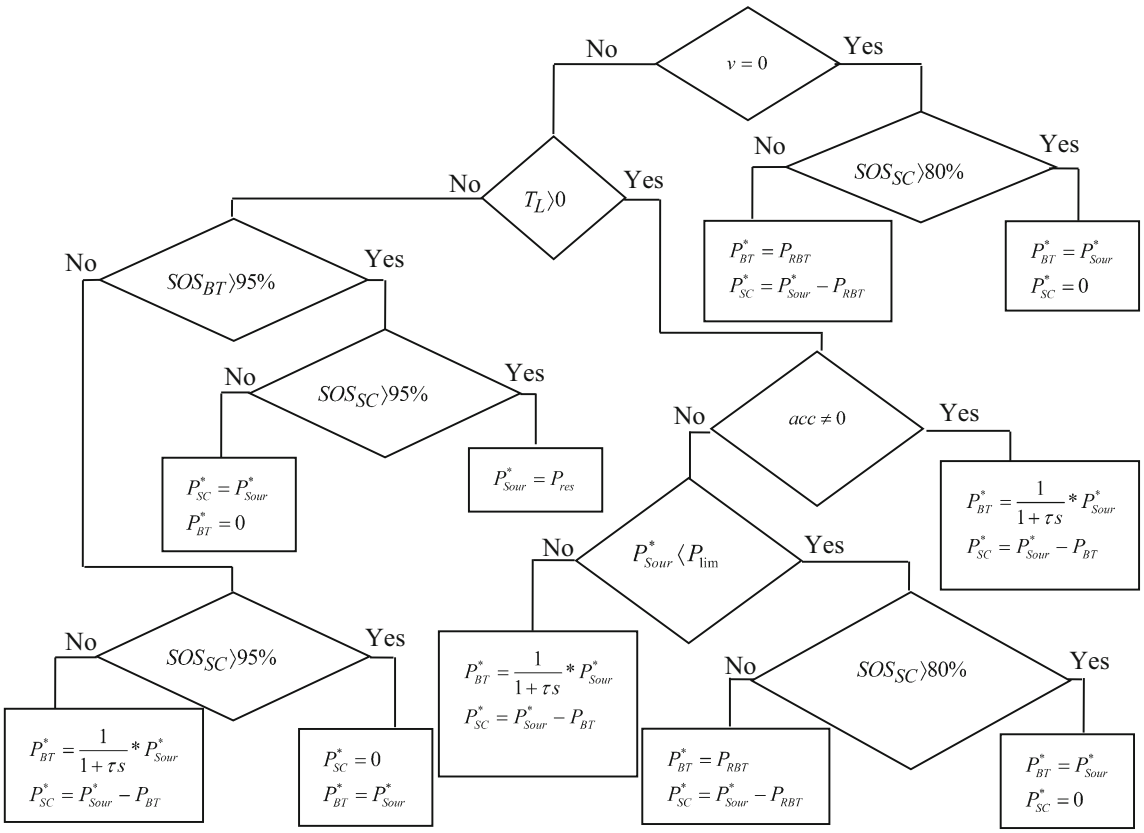

Fig. 6 Flowchart showing the proposed energy management algorithm

of the vehicle is equal to zero and the SOC_{SCs} is below the threshold 80%, then the SCs can be charged with the surplus power of battery, otherwise the $P_{BT} = P_{load}$ and the SCs cannot be charged. If the speed of the vehicle is different from zero, then the sign of the load torque sets the operating mode. For the motor operation, if the acceleration is different from zero a low-pass filter (LPF) is applied to the load power diverting sudden power variation to the supercapacitors:

$$\begin{cases} P^*_{\mathrm{BT}} = \frac{1}{1+\tau S} P^*_{\mathrm{Sour}} \\ P^*_{\mathrm{SC}} = P^*_{\mathrm{Sour}} - P^*_{\mathrm{BT}} \end{cases} \tag{15}$$

Time constant τ of the LPF is fixed considering the dynamic of the batteries as well as supercapacitors size. The latter can fill power gaps during batteries transients (Fig. 5b) [25]. If the acceleration is equal to zero (constant speed), a comparison between the reference source power P^*_{Sour} and the load power limit P_{Lm} is applied; if $P^*_{\mathrm{Sour}} < P_{\mathrm{Lm}}$ and $\mathrm{SOC}_{\mathrm{SCs}} < 80\%$, then the battery uses its rated power to supply both the load and the SCs, otherwise, a LPF is applied to the load power. For the regenerative braking operation, if the SOC of one of the BTs or SCs is less than 95%, then the ESS is directly charged by the load power, if the SOC of both sources is less than 95%, a LPF is applied to the load power as the case of the motor operation where the battery is the main source that absorb the load power. In the case that both batteries and supercapacitors are fully charged (SOC > 95%), a dynamic

Table 4 Simulation parameters

	Storage converters	Load converter
Converter topology	Boost and buck bidirectional converters	Hysteresis inverter
Control technic	Cascade control (PI + hysteresis controller).	Field-oriented control (FOC)
Control parameters (kp, ki), Δi	DC-link voltage controller: (2.12,450)	Speed controller: (227.65, 16100)
	Current_BT: $\Delta i = 1$	Current_inverter: $\Delta i = 1$
	Current_SC: $\Delta i = 1$	
Sample times system: (discrete, Ts $= 5e^{-6}$ s)	DC-link controller: Tc_dc $= 1e^{-5}$s	FOC: $T_{FOC} = 1e^{-5}$s
	Storage controller: Tc_(BT/SC) $= 1e^{-5}$s	Speed controller: Tc_speed $= 5e^{-5}$s

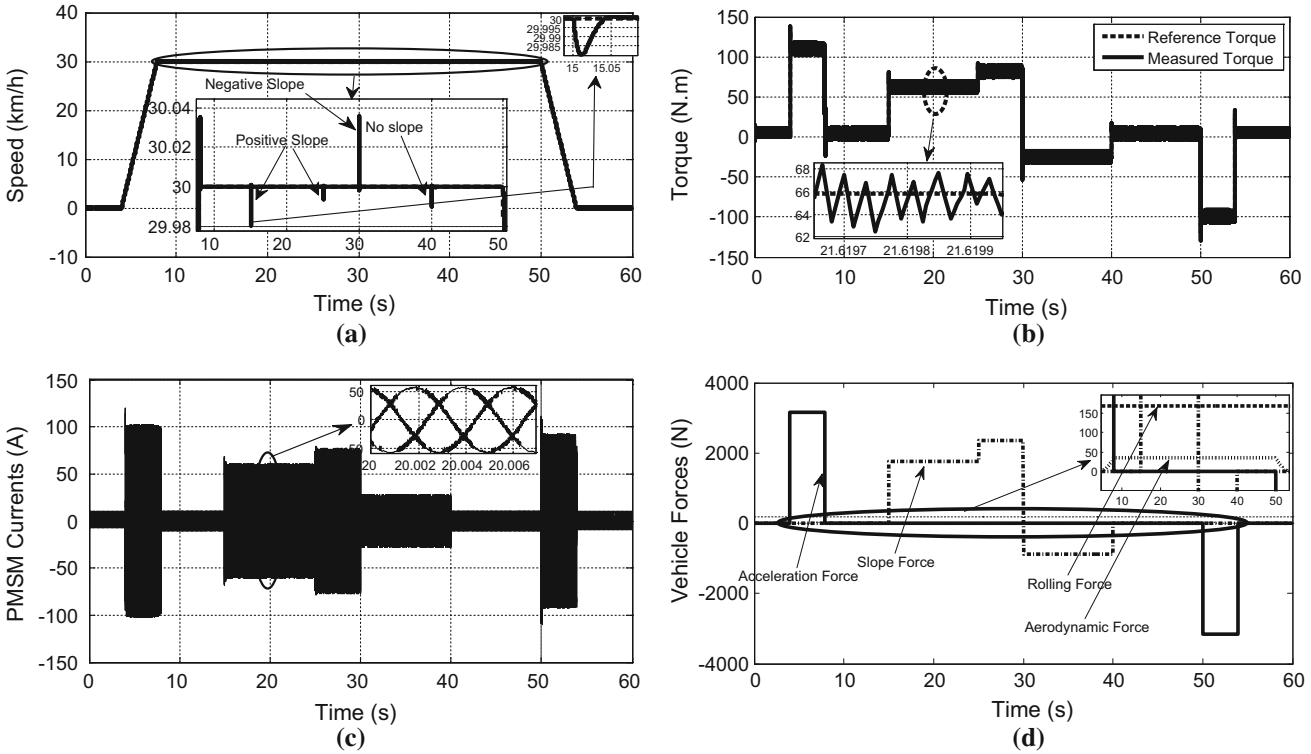

Fig. 7 **a** Linear speed of the vehicle; **b** reference and PMSM torque; **c** motor currents; **d** the tractive forces

braking is used to dissipate the energy of the load. Figure 6 shows the algorithm of the proposed EMS.

5 Simulation results and interpretation

To verify the control of the proposed scheme, a simulation model was built based on Matlab/Simulink software. The simulation parameters are presented in (Table 4).
The vehicle was submitted to a maximum speed of 30 km/h with a 2.135 m/s^2 acceleration; it passes by three phases, an acceleration phase, a phase of constant speed and a deceleration phase. At 15 and 25 s, the car encounters a climbing resistance whose slope is 10 and 13.33%, respectively, then at 30 s the vehicle faces a downhill whose slope is −5%, after 40 s, the car is moving with no slope. It was considered that the battery SOC is 80% and the SCs have a previous charge corresponding to a 190 V voltage.

The vehicle's speed evolution shows a good approximation in time domain to the speed requested, as can be seen in Fig. 7a. The vehicle follows almost perfectly the speed set point, with minor fluctuations. The electromagnetic torque, currents of PMSM and the resistance forces of the vehicle are presented, respectively, in Fig. 7b–d. From Fig. 7d, it is clear that the acceleration and the slope forces present the large proportion of the total tractive effort.

The power waveforms of load and sources, the DC bus voltage, and the SOC of the sources are presented in Fig. 8a–d, respectively.

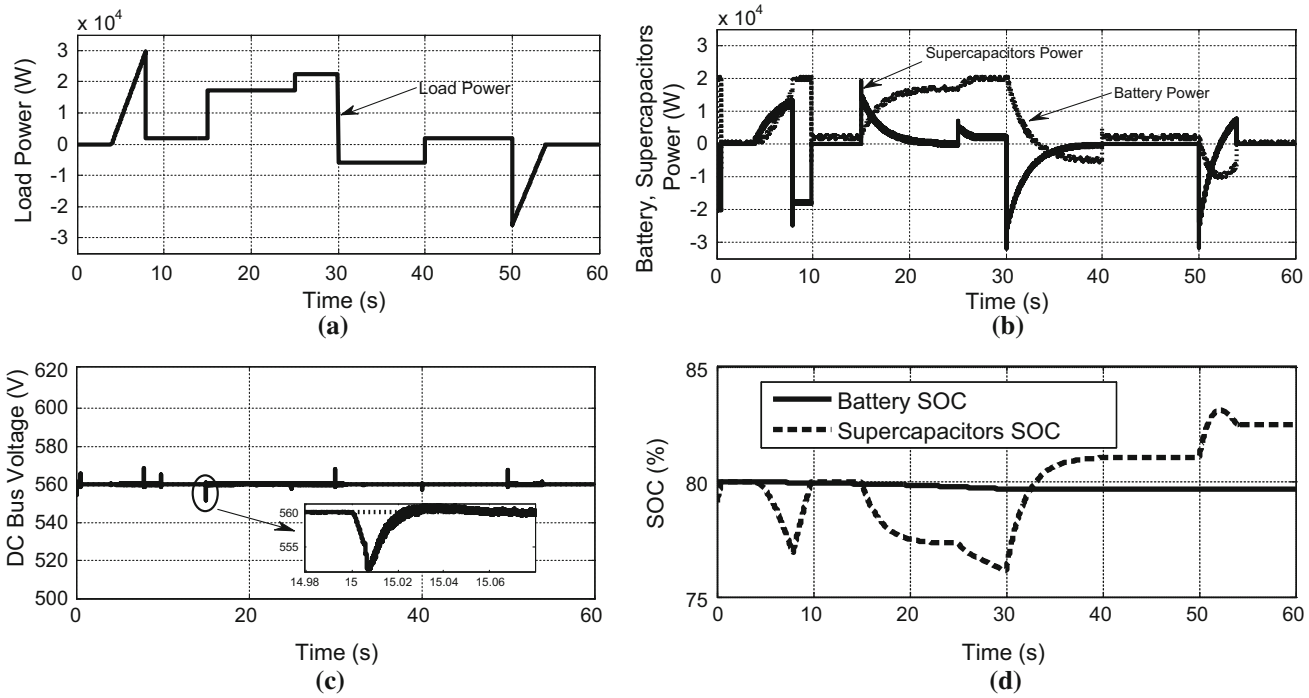

Fig. 8 **a** Power waveform of load, **b** power waveforms of battery and supercapacitors; **c** DC bus voltage; **d** state of charge of the BT and SCs

In the first 4 s, when the vehicle is stopped, the SOC_{SCs} is lower than 80% since sharp acceleration is needed while batteries charge the SCs till its SOC reaches 80%.

At $t = 4$ s, the battery begins to provide power but is not able to reach the reference power, a LPF is applied to the load power and the SCs start to help the battery by providing an extra power .

At $t = 7.9$ s, the car passes slightly the set-point speed with an overshoot then it decreases to its reference thus providing the regenerative braking mode, enabling the supercapacitor to charge, due to its rapid dynamics. After 0.05 s, the vehicle enters the phase of constant speed cruising, the load power is inferior to the limit power and the SOC_{SCs} decreases to lower than 80%, the battery shares its power between the load and the supercapacitors. It is easy to observe that the SCs power becomes negative, it means that the SCs receive some power from the battery and recharges while the EV is moving. At $t = 15$ s the vehicle encounters a slope resistance, the load torque increases, the vehicle speed recovers fast and goes back to the reference speed. The current reference rises to about 57 A to generate a higher electromagnetic torque (Fig. 7b, c) to maintain desired speed, the battery is then subjected to a rising power request from the load, a LPF is applied to the load power diverting sudden power variation to the supercapacitors while the two DC–DC converters work in boost-mode. After this transient phase the battery supplies a full load power and the LPF operation is canceled. At $t = 25$ s while the slope resistance increases, the battery reaches its rated power of 20 kW; the supercapacitor provides more energy to achieve the torque required.

At $t = 30$ s, the vehicle encounters a downhill slope, thus the load torque becomes negative; the system passes into regenerative braking mode and reversal of the current flow through the motor takes place. The SCs respond directly to the needs of the load by absorbing current peaks as requested by the EMS and the kinetic energy of the EV is transformed in electrical energy which is stored in the battery. At $t = 40$ s, when the downhill slope disappears, the SOC_{SCs} is higher than 80%, and the battery supplies the motor alone. At $t = 50$ s, the EV starts to decelerate until it stops. The motor acts as a generator driven by the vehicle's wheels. The load power is distributed between both power sources according to the law of energy conservation with the battery being the main energy source. At $t = 54$ s, the battery power is equal to the reference power thus the supercapacitor is no more needed. DC bus voltage (Fig. 8c) remained stable during the simulation; however, there were some brief peaks during the quick transitions of the load power. It may be noted that the SOC_{BT} varies slowly and the SOC_{SCs} varies rapidly while remaining high depending on the EMS (Fig. 8d).

A simulation is developed using urban drive cycle ECE-15 to test the energy storage system using the proposed EMS. In Fig. 9, the speed, power sharing, SOC and sources energy are presented.

Batteries supply the average power requested by the EV load and receive energy while in braking phase. During

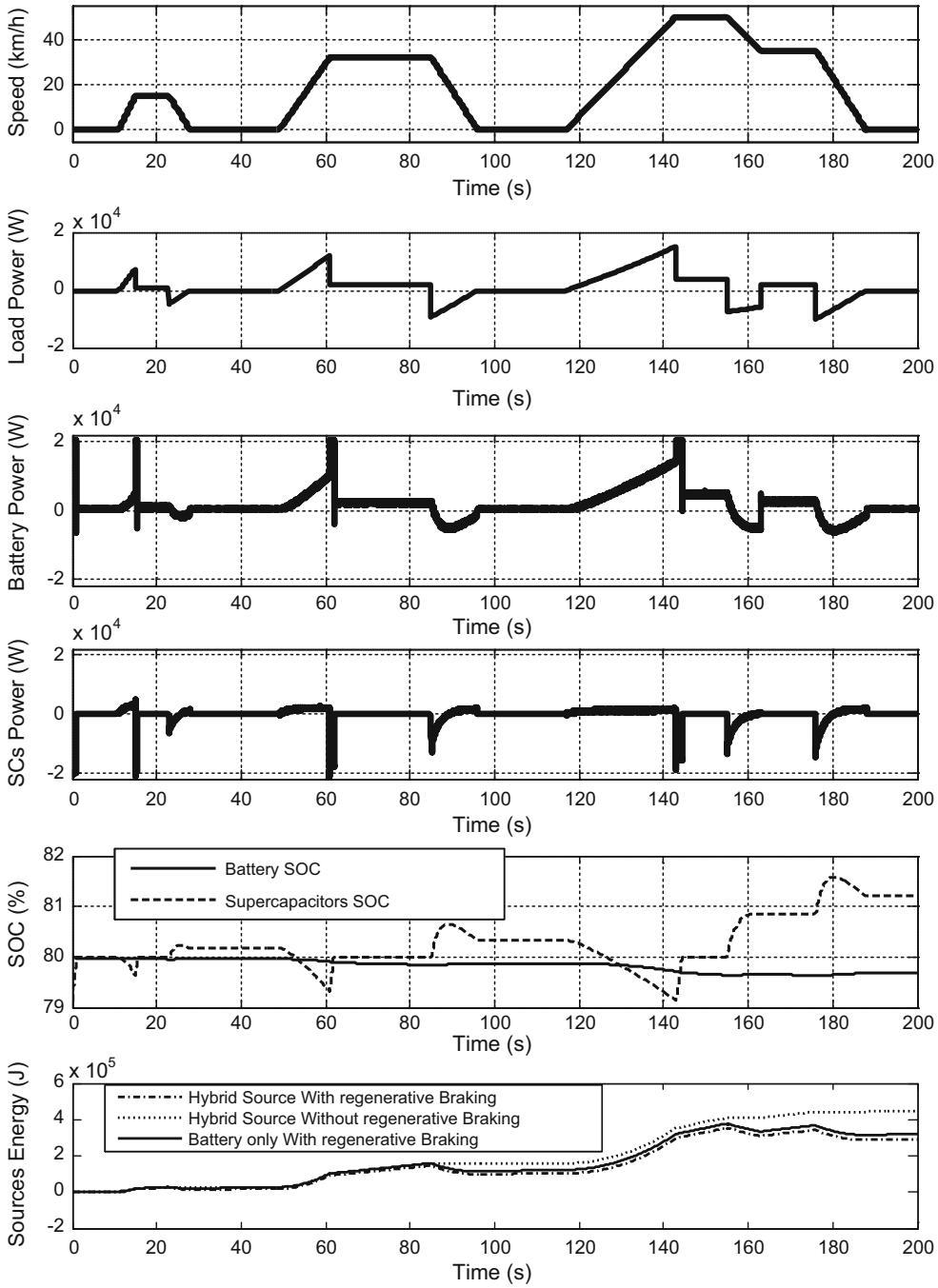

Fig. 9 Simulation of an urban drive cycle ECE-15

accelerations and decelerations phases SCs assist batteries. Moreover SCs receive energy from the batteries when their SOC is below the minimum threshold in order to restore a minimum energy level to help the batteries in the next accelerations and braking phases. The EV reaches the end of the cycle maintaining a high level of energy in its main and auxiliary sources ($SOC_{BT} = 79.68\%$, $SOC_{SCs} = 81.2\%$).

The results indicate that the energy required to move the EV using the drive cycle ECE15 without using regenerative braking is 445 KJ. This energy consumption is calculated by integrating the sum of the power output at the battery and supercapacitors terminals during the whole cycle. Meanwhile when using the regenerative braking only 289 KJ is needed. On the other hand a 319 KJ is necessary when using battery alone with regenerative braking. These results show the effectiveness of the proposed EMS.

6 Conclusion

In this work we presented a new strategy of an energy management between battery and supercapacitors for an electric vehicle by exploiting the advantages of each source. The goal of this energy management is to increase the autonomy of the vehicle by recovering the energy in the phases of decelerations or downhills and increase the lifetime of batteries by the integration of supercapacitors. The proposed strategy distributes the regulation of DC bus voltage to both sources depending on the needs of the load. This enables efficient energy management. During the transitions of the power load, the SCs directly respond to the needs of the load by providing or absorbing power peaks as requested by the EMS. The simulation results show that the proposed EMS permits to the SCs to have high SOC, allowing for better energy management and provide an extended EV range.

References

1. Nouh A (2008) Contribution au développement d'un simulateur pour les véhicules électriques routiers. Dissertation, the University of Technology of Belfort-Montbéliard
2. Trovão JP, Pereirinha PG, Jorge HM (2009) Simulation model and road tests comparative results of a small urban electric vehicle. In: 35th annual conference on IEEE industrial electronics, Porto, pp 836–841. doi:10.1109/IECON.2009.5415028
3. Alireza K, Zhihao L (2010) Battery, ultracapacitor, fuel cell, and hybrid energy storage systems for electric, hybrid electric, fuel cell, and plug-in hybrid electric vehicles: state of the art. IEEE Trans Veh Technol 59:2806–2814. doi:10.1109/TVT.2010.2047877
4. Trovão JP, Pereirinha PG, Jorge HM, Antunes CH (2013) A multi-level energy management system for multi-source electric vehicles—An integrated rule-based meta-heuristic approach. Appl Energy 105:304–318. doi:10.1016/j.apenergy.2012.12.081
5. Long B, Lim ST, Bai ZF, Ryu JH, Chong KT (2014) Energy management and control of electric vehicles using hybrid power source in regenerative braking operation. Energies 7:4300–4315. doi:10.3390/en7074300
6. Ben Salah I, Bayoudhi B, Diallo D (2014) EV energy management strategy based on a single converter fed by a hybrid battery/supercapacitor power source. In: First international conference on green energy ICGE, Sfax: IEEE, pp 246–250. doi:10.1109/ICGE.2014.6835429
7. Trovão JP, Santos VDN, Pereirinha PG, Jorge HM (2013) A simulated annealing Approach for optimal power source management in a small EV. IEEE Trans Sustain Energy 4:867–876. doi:10.1109/TSTE.2013.2253139
8. Lahyani A, Venet P, Guermazi A, Troudi A (2013) Battery/supercapacitors combination in interruptible power supply. IEEE Trans Power Electron 28:1509–1522. doi:10.1109/TPEL.2012.2210736
9. Armenta J, Núñez C, Visairo N, Lázaro I (2015) An advanced energy management system for controlling the ultracapacitor discharge and improving the electric vehicle range. J Power Sour 284:452–458. doi:10.1016/j.jpowsour.2015.03.056
10. Yoong MK, Gan YH, Gan GD, Leong CK (2010) Studies of regenerative braking in electric vehicle . In: Sustainable utilization and development in engineering and technology. IEEE, Petaling Jaya. pp 40–45. doi:10.1109/STUDENT.2010.5686984
11. Sun H, Pei X, Xu L, Wang H, Sheng Y, Yu Y(2012) Application of battery ultracapacitor hybrid system in the hybrid electric vehicles. In: Proceedings of the FISITA 2012 world automotive congress, Springer, Berlin, pp 785–793. doi:10.1007/978-3-642-33741-3_7
12. Zhou HB, Long B, Coa BG (2013) New energy recovery H∞ robust controller for electric bicycles. Int J Automot Technnol 14:283–289. doi:10.1007/s12239-013-0032-0
13. Victor M (2007) Conception Optimale Systémique des Composants des Chaines de Traction Electrique. Dissertation, Ecole Centrale de Lille
14. Tremblay O, Dessaint LA (2009) Experimental validation of a battery dynamic model for EV applications. World Electr Veh J 3:289–298
15. Shuhui L, Ke B, Xingang F, Huiying Z (2014) Energy management and control of electric vehicle charging stations. Electr Power Compon Syst 42(3–4):339–347. doi:10.1080/15325008.2013.837120
16. Perdigao MS, Trovao JP, Alonso JM, Pereirinha PG, Saraiva ES(2013) Experimental large-signal characterization of power inductors in bidirectional electric vehicle DC–DC converters for simulation analysis. In: Power electronics and applications conference. IEEE, Lille. pp 1–10. doi:10.1109/EPE.2013.6634438
17. Silva MA, Trovão JP, Pereirinha PG (2011) Implementation of a multiple input DC–DC converter for electric vehicle power system. In: Proceedings of 3rd international youth conference energetics (IYCE). IEEE, Leiria, pp 1–8
18. Baussière R, Labrique F, Seguier G (1997) les convertisseurs de l'électronique de puissance. Tec & Doc Lavoisier, France
19. Trovão JP, Santos VDN, Antunes CH, Pereirinha PG (2015) A real-time energy management architecture for multi-source electric vehicles. IEEE Trans Ind Electron 62:3223–3233. doi:10.1109/TIE.2014.2376883
20. Paire D, Simoes M G, Lagorse J, Miraoui A (2010) A real-time sharing reference voltage for hybrid generation power system. In: Industry applications society annual meeting (IAS). IEEE, Houston. pp 1–8. doi:10.1109/IAS.2010.5615382
21. Victor P (2013) Electrothechnical systems simulation with simulink and simpowersystems. CRC Press, Boca Raton
22. Yusivar F, Hidayat N, Gunawan R, Halim A (2014) Implementation of field oriented control for permanent magnet synchronous motor. In: IEEE international conference on electrical engineering and computer science. Kuta, pp 359–362, doi:10.1109/ICEECS.2014.7045278
23. Azizi I, Radjeai H (2015) A bidirectional DC-DC converter fed DC motor for electric vehicle application. In: 4th international conference on electrical engineering (ICEE). IEEE, Boumerdes. pp 1–5. doi:10.1109/INTEE.2015.7416683
24. James L, John L (2003) Electr Veh Technol Explain. Wiley, Hoboken
25. Choudar A, Boukhetala D, Barkat S, Brucker J (2014) A local energy management of a hybrid PV-storage based distributed generation for microgrids. Energ Convers Manag 90:21–33. doi:10.1016/j.enconman.2014.10.067